(Submitted for possible publication in *International Journal of Mechanical Science*)

Maximizing the Fundamental frequency of Laminated Cylindrical Panels using Layerwise Optimization

Y. Narita
Department of Mechanical Engineering, Hokkaido University
Sapporo 060-8628, Japan
and
P. Robinson
Aeronautics Department, Imperial College London
London SW7 2AZ, UK

This manuscript has been neither published nor currently submitted for publication either in a serial, professional journal or as a part in a book.

Number of copies submitted 3
Number of manuscript pages 15
Number of figures 4
Number of tables 6

Mailing Address: Prof. Y. Narita, Department of Mechanical Engineering
School of Engineering, Hokkaido University
N-13, w-8, Kitaku, Sapporo, 060-8628, Japan
ynarita@eng.hokudai.ac.jp, fax: +81-11-706-7889

(abstract)

A method of analysis is presented for determining the free vibration frequencies of cylindrically curved laminated panels under general edge conditions, and is implemented in a layerwise optimization (LO) scheme to determine the optimum fiber orientation angles for the maximum fundamental frequency. Based on the classical lamination theory applicable to thin panels, a method of Ritz is used to derive a frequency equation wherein the displacement functions are modified to accommodate arbitrary sets of edge conditions for both in-plane and out-of-plane motions. The LO approach, a recently developed scheme for laminated plates, is extended for the first time to the optimum design of curved panels. In a number of numerical examples, the accuracy of the analysis and the effectiveness of the LO approach are demonstrated.

Keywords: Optimum design, Laminated composite, Cylindrical panel, Frequency design

1. INTRODUCTION

Much progress has been made over the last two decades in the development of increasingly more efficient composite structures and industries continue to investigate strategies for fully exploiting the potential of composites for a variety of structural forms including the laminated cylindrical panel which is the subject of this paper. Given that a key advantage of composite laminates, in addition to their potential for high specific stiffness and strength, is the ability to tailor the properties of the laminate through lay-up design then it is clearly appropriate that efforts be applied to fully optimize this tailoring process.

A curved panel is one form of general shells and falls into a category of shallow shell, and the vibration analysis of shallow shells has a long history of academic and practical interest, as summarized in a monograph [1] by Leissa and in review papers by Qatu [2] and Liew, Lim and Kitipornchai [3]. A cylindrically curved panel can be regarded as a shallow shell that has small curvature (i.e., large curvature radius) in one direction. In reference [4], a complete set of equations for elastic deformation of laminated composite shallow shells are presented for static and vibration behaviors.

For vibration of laminated composite curved panels, some relevant important discussions were found in the publications in the 1980's. Bert and Kumar [5] formulated vibration of the panel considering the bimodulus behaviors. Soldatos compared some shell theories for the analysis of cross-ply laminated panels [6] and studied influence of thickness shear on the vibration of antisymmetric angle-ply panels [7].

Recently, Lam and Chun [8] dealt with dynamic analysis of clamped laminated curved panels and Berçin [9] obtained natural frequencies of cross-ply laminated curved panels. In 1997, Bardell, Dunsdon and Langley [10] presented free and forced vibration analysis of cylindrically curved laminated panels and Selmane and Lakis [11] also analyzed anisotropic cylindrical shells. More recently, Soldatos and Messina [12] studied the influence of boundary conditions and transverse shear on the vibration of angle-ply laminated cylindrical panels. Kabir [13] applied a shallow shell theory of Reissner to determine the response of cylindrical panels with arbitrary lay-ups, and a mesh free approach was used by Zhao, Liew and Ng [14] to analyze the vibration response of laminated cylindrical panels.

As for tailoring, Raouf [15] considered the effect of tailoring on the dynamic characteristics

of composite panels using fiber orientation. Narita, Ito and Zhao [16] applied a genetic algorithm to determine the maximum fundamental frequency of laminated shallow shells that are supported by shear diaphragms and for the same problem they used Kuhn-Tucker condition to derive the maximum fundamental frequency of laminated shallow shells [17]. The effect of using various solutions upon optimizing vibration characteristics of laminated shallow shells are also studied [18]. These papers [15-18] are however limited to a simple case with the edges fully supported by shear diaphragms where a simplified frequency formula is derivable by neglecting the cross-elasticity terms.

In the present paper, a semi-analytical solution is presented for the free vibration of cylindrically curved laminated panels with arbitrary boundary conditions with respect to in-plane and out-of-plane displacements. The solution is based on a method of Ritz wherein the displacement functions are modified by boundary indices [19] to satisfy the required kinematical boundary conditions.

Furthermore the analytical method is combined with the layerwise optimization (LO) scheme, recently developed for laminated flat plates [20][21]. Numerical examples demonstrate the accuracy of the present Ritz solution to determine natural frequencies of cylindrically curved panels with various edge conditions, and also the extension of the LO approach to the curved panels is shown to be quite effective in obtaining the optimum fiber orientation angles which maximize the fundamental frequencies of the laminated panels.

2. ANALYSIS

The quadratic mid-surface of a shallow shell (panel) may be expressed in a rectangular coordinate system as

$$\phi(x,y) = -\frac{1}{2}\left(\frac{x^2}{R_x} + 2\frac{xy}{R_{xy}} + \frac{y^2}{R_y}\right) \tag{1}$$

where R_x and R_y are the radii of curvature in the x and y directions, respectively, and R_{xy} is the radius of twist. For a cylindrically curved panel, the orientation of the xy coordinates may be chosen so that $R = R_x$ is a principal constant curvature radius and R_y and R_{xy} are infinite, as shown in Fig.1. The dimension of its planform is given by $a \times b$ and the panel thickness is h. The four sides are subjected to uniform in-plane (i.e., stretching) and out-of-plane (bending)

Fig.1

boundary conditions.

Using the Kirchhoff hypothesis, the displacements $u^*(x,y,z,t)$, $v^*(x,y,z,t)$ and $w^*(x,y,z,t)$ of an arbitrary point in a panel are written as

$$u^* = u - z\frac{\partial w}{\partial x},\quad v^* = v - z\frac{\partial w}{\partial y},\quad w^* = w \tag{2}$$

where z is the coordinate measured from the mid-surface in the direction of outer normal. The $u(x,y,t)$ and $v(x,y,t)$ are displacement components, tangent to the mid-surface and parallel to the xz and yz planes, respectively, and $w(x,y,t)$ is a displacement component normal to the mid-surface at a typical point on the mid-surface.

In the linear theory, the strain components at an arbitrary point (x,y,z) are

$$\varepsilon_x^* = \varepsilon_x + z\kappa_x,\quad \varepsilon_y^* = \varepsilon_y + z\kappa_y,\quad \gamma_{xy}^* = \gamma_{xy} + z\kappa_{xy} \tag{3}$$

assuming that z is negligible in comparison with R, where the membrane strains are given by

$$\varepsilon_x = \frac{\partial u}{\partial x} + \frac{w}{R},\quad \varepsilon_y = \frac{\partial v}{\partial y},\quad \gamma_{xy} = \frac{\partial v}{\partial x} + \frac{\partial u}{\partial y} \tag{4}$$

and the curvature changes due to the vibratory displacements are

$$\kappa_x = -\frac{\partial^2 w}{\partial x^2},\quad \kappa_y = -\frac{\partial^2 w}{\partial y^2},\quad \kappa_{xy} = -2\frac{\partial^2 w}{\partial x \partial y} \tag{5}$$

The kinetic approximations (2)-(5) used in the present shallow shell analysis are those of the Donnell type [4].

For a laminated panel composed of fibrous composite thin layers, each layer may be regarded as a macroscopically orthotropic but the fiber orientation may not be parallel to the coordinate axes. The stress-strain equations for an element of material in the k th layer can be written as

$$\begin{Bmatrix} \sigma_x \\ \sigma_y \\ \tau_{xy} \end{Bmatrix}^{(k)} = \begin{bmatrix} \bar{Q}_{11} & \bar{Q}_{12} & \bar{Q}_{16} \\ \bar{Q}_{12} & \bar{Q}_{22} & \bar{Q}_{26} \\ \bar{Q}_{16} & \bar{Q}_{26} & \bar{Q}_{66} \end{bmatrix}^{(k)} \begin{Bmatrix} \varepsilon_x \\ \varepsilon_y \\ \gamma_{xy} \end{Bmatrix} \tag{6}$$

where the constants $\bar{Q}_{ij}^{(k)}$ are the elastic constants of the k th layer. The $\bar{Q}_{ij}^{(k)}$ are determined from the transformation relationships using the fiber orientation angle θ and the stiffness

$$Q_{11} = \frac{E_L}{1-\nu_{LT}\nu_{TL}},\quad Q_{12} = \nu_{TL}Q_{11},\quad Q_{22} = \frac{E_T}{1-\nu_{LT}\nu_{TL}},\quad Q_{66} = G_{LT} \tag{7}$$

where E_{L} and E_{T} are the moduli of elasticity in the L and T directions, respectively, G_{LT} is the

shear modulus and ν_{LT} and ν_{TL} are the major and minor Poisson's ratios in an orthotropic layer. The transformation relationship (6) is found in well-known textbooks [22, 23].

The force resultants and the moment resultants are obtained by integrating the stresses and the stresses multiplied by z, respectively, over the panel thickness h, and are written in matrix form as

$$\begin{Bmatrix} N \\ M \end{Bmatrix} = \begin{bmatrix} A & B \\ B & D \end{bmatrix} \begin{Bmatrix} \varepsilon \\ \kappa \end{Bmatrix} \tag{8}$$

where $\{N\}$, $\{M\}$, $\{\varepsilon\}$ and $\{\kappa\}$ are the vectors of force resultants, moment resultants, mid-surface strains and curvatures, respectively, given by

$$\{N\} = \begin{Bmatrix} N_x \\ N_y \\ N_{xy} \end{Bmatrix}, \quad \{M\} = \begin{Bmatrix} M_x \\ M_y \\ M_{xy} \end{Bmatrix}, \quad \{\varepsilon\} = \begin{Bmatrix} \varepsilon_x \\ \varepsilon_y \\ \gamma_{xy} \end{Bmatrix}, \quad \{\kappa\} = \begin{Bmatrix} \kappa_x \\ \kappa_y \\ \kappa_{xy} \end{Bmatrix} \tag{9a,b,c,d}$$

and $[A]$,$[B]$ and $[D]$ are the matrices of stiffness coefficients defined by

$$[A] = \begin{bmatrix} A_{11} & A_{12} & A_{16} \\ A_{12} & A_{22} & A_{26} \\ A_{16} & A_{26} & A_{66} \end{bmatrix}, \quad [B] = \begin{bmatrix} B_{11} & B_{12} & B_{16} \\ B_{12} & B_{22} & B_{26} \\ B_{16} & B_{26} & B_{66} \end{bmatrix}, \quad [D] = \begin{bmatrix} D_{11} & D_{12} & D_{16} \\ D_{12} & D_{22} & D_{26} \\ D_{16} & D_{26} & D_{66} \end{bmatrix} \tag{10a,b,c}$$

The stiffness coefficients in Eqs.(10a,b,c) are determined by

$$A_{ij} = \sum_{k=1}^{K} \bar{Q}_{ij}^{(k)} \left(z_k - z_{k-1} \right), \quad B_{ij} = \frac{1}{2} \sum_{k=1}^{K} \bar{Q}_{ij}^{(k)} \left(z_k^2 - z_{k-1}^2 \right), \quad D_{ij} = \frac{1}{3} \sum_{k=1}^{K} \bar{Q}_{ij}^{(k)} \left(z_k^3 - z_{k-1}^3 \right) \tag{11a,b,c}$$

(i,j=1,2,6) where z_k is the distance from the mid-surface to the upper surface of the k th layer and K is the total number of layers [22][23].

In the present study, the free vibration problem can be solved by means of the Ritz method. This requires the evaluation of energy functional. The strain energy stored in a panel during elastic deformation is written in the classical (thin) shallow shell theory by

$$V = V_s + V_{bs} + V_b \tag{12}$$

where V_s, V_{bs} and V_b are the parts of the total strain energy due to stretching, bending-stretching coupling and bending, respectively:

$$V_s = \frac{1}{2} \iint \{\varepsilon\}^T [A] \{\varepsilon\} \, dArea \,, \tag{13a}$$

$$V_{bs} = \frac{1}{2} \iint \left(\{\kappa\}^T [B] \{\varepsilon\} + \{\varepsilon\}^T [B] \{\kappa\} \right) dArea \tag{13b}$$

$$V_b = \frac{1}{2}\iint \{\kappa\}^T [D]\{\kappa\}\, dArea \tag{13c}$$

The kinetic energy of the panel due to translational motion only is given by

$$T = \frac{1}{2}\rho\iint \left[\left(\frac{\partial u}{\partial t}\right)^2 + \left(\frac{\partial v}{\partial t}\right)^2 + \left(\frac{\partial w}{\partial t}\right)^2\right] dArea \tag{14}$$

where ρ is the average mass density of the panel per unit area of the mid-surface.

For clarity in the formulation, the following dimensionless quantities are introduced.

$$\xi = \frac{2x}{a},\ \ \eta = \frac{2y}{b} \quad \text{(dimensionless coordinates)} \tag{15a}$$

$$\Omega = \omega a^2\sqrt{\frac{\rho}{D_0}} \quad \text{(dimensionless frequency parameter)} \tag{15b}$$

$$\text{with}\ \ D_0 = \frac{E_T h^3}{12\left(1-\nu_{LT}\nu_{TL}\right)} \quad \text{(reference plate stiffness)} \tag{15c}$$

In the Ritz method the displacements may be assumed in the form

$$u(\xi,\eta,t) = \sum_{i=0}^{M-1}\sum_{j=0}^{N-1} P_{ij} X_i(\xi) Y_j(\eta) \sin\omega t \tag{16a}$$

$$v(\xi,\eta,t) = \sum_{k=0}^{M-1}\sum_{l=0}^{N-1} Q_{kl} X_k(\xi) Y_l(\eta) \sin\omega t \tag{16b}$$

$$w(\xi,\eta,t) = \sum_{m=0}^{M-1}\sum_{n=0}^{N-1} R_{mn} X_m(\xi) Y_n(\eta) \sin\omega t \tag{16c}$$

where P_{ij}, Q_{kl} and R_{mn} are unknown coefficients and $X_i(\xi)$, $Y_j(\eta)$, .. and $Y_n(\eta)$ are the functions that satisfy at least the kinematical boundary conditions at the edges. The upper limit in each of the summations (16) is arbitrary but is unified here for simplicity in the convergence test.

After substituting Eqs.(16) into the functional *L*

$$L = T_{max} - V_{max} \tag{17}$$

composed of the maximum strain and kinetic energies obtained from Eqs.(12) and (14), the stationary value is obtained by

$$\frac{\partial L}{\partial P_{ij}} = 0,\ \ \frac{\partial L}{\partial Q_{kl}} = 0,\ \ \frac{\partial L}{\partial R_{mn}} = 0$$

$$(i,k,m=0,1,2,..,(M-1);\ j,l,n=0,1,2,...,(N-1)) \qquad \text{(18a) (18b) (18c)}$$

The result of the minimization process (18) yields a set of homogeneous, linear simultaneous equations in the unknowns $\{P_{ij},Q_{kl},R_{mn}\}$. For non-trivial solutions the determinant of the coefficient matrix is set to zero. The $(M\times N)\times 3$ eigenvalues may be extracted and the lowest several eigenvalues (natural frequencies) are important from a practical viewpoint.

The above procedure is a standard routine of the Ritz method, and is modified to incorporate arbitrary edge conditions [19]. This approach introduces the following polynomials

$$X_i(\xi)=\xi^i(1+\xi)^{Bu1}(1-\xi)^{Bu3},\ \ Y_j(\xi)=\eta^j(1+\eta)^{Bu2}(1-\eta)^{Bu4} \qquad \text{(19a)(19b)}$$

$$X_k(\xi)=\xi^k(1+\xi)^{Bv1}(1-\xi)^{Bv3},\ \ Y_l(\eta)=\eta^l(1+\eta)^{Bv2}(1-\eta)^{Bv4} \qquad \text{(19c)(19d)}$$

$$X_m(\xi)=\xi^m(1+\xi)^{Bw1}(1-\xi)^{Bw3},\ \ Y_n(\eta)=\eta^n(1+\eta)^{Bw2}(1-\eta)^{Bw4} \qquad \text{(19e)(19f)}$$

where B_{rs} $(r=u,v,w;\ s=1,2,3,4)$ is the boundary index [19] which is used to satisfy the kinematic boundary conditions. The capital letter *B* stands for Boundary. The first subscript letter in B_{rs} indicates which displacement (*u*,*v* or *w*) is dealt with and the second subscript number indicates which edge, Edge(1),.. or Edge(4), is under consideration. The Edge(1),(2),(3) and (4) denote the boundary along $x=-a/2$, $y=-b/2$, $x=a/2$ and $y=b/2$, respectively (See Fig.1).

For in-plane displacements *u* and *v*, B_{rs}=0 $(r=u,v;\ s=1,2,3,4)$ denote that the specified displacement along the specified edge is free and B_{rs}=1 denote that the displacement is rigidly fixed. For out-of-plane displacement *w*, B_{rs}=0, 1 and 2 $(r=w;\ s=1,2,3,4)$ denote that the specified displacement along the specified edge is free, simply supported and clamped, respectively. With such boundary indices, one can accommodate arbitrary sets of both in-plane and out-of-plane boundary conditions in the vibration analysis and computation.

The introduction of the boundary index makes it possible to deal with a tremendous number of edge conditions in the analysis. The number of combinations in the boundary condition is $(2\times 2\times 3)^4$ =20736, when one of the two conditions (free or fixed) in *u* and *v* and one of the three conditions (free, simply supported or clamped) in *w* are imposed along each of the four edges.

This is significantly larger than the *plate* analysis [19] where only out-of-plane displacement is concerned for bending vibration of symmetrically laminated plates. The present vibration analysis can calculate natural frequencies for any of these combinations.

In the following numerical examples, however, the boundary conditions are limited to those similar to the standard plate boundary conditions, such as free edge, simply supported edge and clamped edge. For example, at the Edge (1) along $x=-a/2$

$B_{u1}= B_{v1}= B_{w1}=0$ for the free edge (no constraint), denoted by F

$B_{u1}=0, B_{v1}=1, B_{w1}=1$ for the simply supported edge (S2 type condition), by S (20)

$B_{u1}= B_{v1}=1, B_{w1}=2$ for the clamped edge (fully constrained edge), by C

3 DESIGN PROBLEM AND LAYERWISE OPTIMIZATION

An optimum structural design is generally composed of two parts: the structural analysis and the optimization process. The first part has been developed in Sec.2 and the second part is formulated here. The object function for optimization is taken to be a frequency parameter Ω defined in Eq.(15b) and is denoted by Ω_1 for the fundamental mode. The term "fundamental frequency" indicates the lowest eigenvalue for given conditions.

The design variables are taken to be a set of fiber orientation angles in the K layers of the upper (or lower) half of the plate cross-section:

$$[\theta_1/\theta_2/\ldots/\theta_k/\ldots/\theta_K]_S \tag{21}$$

where θ_k is the fiber orientation angle of the k th layer (k=1:outermost, k=K: innermost) and the subscript "s" denotes symmetric lamination. Therefore, the optimization problem may be written in standard mathematical form as

$$\begin{aligned} &\text{Find : } \vec{\theta} = (\theta_1,\theta_2,\ldots,\theta_K) \\ &\text{which maximizes : } \Omega_1 = \Omega_1\left(\vec{\theta}\right) \\ &\text{subject to the constraints: } -90^\circ \le \theta_k \le 90^\circ \quad (k=1,2,\ldots,K) \end{aligned} \tag{22}$$

It is known that the approach of using each fiber orientation angle directly as a design variable is straightforward but the number of design variables increases in proportion to the number of layers, resulting in a multi-dimensional search optimization problem. The layerwise optimization (LO) procedure makes use of a simple physical observation [20][21] that in the bending of plates, the outer layer has a greater stiffening effect than an inner layer and therefore

has a greater influence on the natural frequency. This physical fact suggests that the outer layer plays a more influential role in determining the maximum natural frequency of laminated curved panel. It is intended here to extend the LO approach, already successfully used for plate optimization, to the panel problems with slight curvature.

Therefore, the following approach to the solution of the optimization problem is advocated.

The optimum stacking sequence $[\theta_1/\theta_2/\ldots/\theta_K]_{S,opt}$ *for the maximum (fundamental) natural frequency of a laminated panel can be obtained by determining the optimum fiber angle for each layer sequentially working from the outermost to the innermost layer*.

The difference between the flat plate problems [20] [21] and the present cylindrical panel problem is that the in-plane motion is coupled with the out-of-plane motion and the use of the outer layer stiffness as a key influential variable may not be effective to the in-plane motion. Due to this difference the applicability of the LO procedure to the present problem is questionable, but it will be demonstrated that the LO procedure works quite effectively for shallow cylindrical panels because the bending is still dominant in the vibration of these panels.

When $\Omega^{(k)}_{opt}$ is assumed to be the maximum value of the frequency parameter obtained in the *k* th step (Note that the same *k* indicating the layer number is used because it deals with the *k* th layer), the following procedure, based on the foregoing assumption, may be used to determine $\Omega_{1,opt}$:

Step 0: Assume a laminated panel made of *K* hypothetical layers in the upper (lower) half of the cross-section with mass but no rigidity.

Step 1: Find $\theta_{1,opt}$, using a one-dimensional search with a certain increment in θ, which determines the maximum fundamental frequency $\Omega^{(1)}_{opt}$ of the laminated panel with an orthotropic lamina (i.e., with E_L, E_T, G_{LT} and ν_{LT}) in the first outermost layer. The (*K*-1) inner layers remain hypothetical with no rigidity.

Step 2: Find $\theta_{2,opt}$, using a one-dimensional search, which gives $\Omega^{(2)}_{opt}$ of the laminated panel with an orthotropic lamina in the second layer and an orthotropic first layer with $\theta_1=\theta_{1,opt}$. The inner (*K*-2) layers remain hypothetical with no rigidity.

Step 3 to *K*-1: The foregoing process is repeated to yield $\theta_{3,opt},\ldots\theta_{(K-1),opt}$.

Step *K*: Find $\theta_{K,opt}$ which gives $\Omega^{(K)}_{opt}$ of the laminated panel with an orthotropic lamina

in the *K*-th innermost layer. This last step determines the optimum lay-up $[\theta_1/\theta_2/\ldots/\theta_K]_{S,opt}$ which yields the maximum fundamental frequency $\Omega_{1,opt}=\Omega^{(K)}_{opt}$ of the panel.

In Reference [20] where the idea of LO procedure was first presented, the layers located inner than the optimized layer were assumed isotropic with Young's modulus E_T in all directions. However, this assumption is not physically valid (i.e., the relation of $E_L \nu_{TL}=E_T \nu_{LT}$ is broken), and is replaced by the idea of "hypothetical layer with no rigidity but with mass".

The above set of Steps 1-*K* is considered as one cycle of the LO iterative solution procedure [21]. In the first cycle, the inner layers are initially assumed to have zero stiffness, and the fiber orientation angles determined at Step *K* in the first cycle, i.e. $[\theta_1/\theta_2/\ldots/\theta_K]_{S,opt}$, must be a better initial approximation for the second cycle of Steps 1-*K*. The iterative cycles continue until a converged solution is obtained. The flow chart is given in Fig.2 to define the above algorithm in concise manner.

Fig.2

4 REULTS AND DISCUSSIONS

Numerical examples are given for symmetrically laminated, 8-layer cylindrical panels with square (*a/b*=1) and rectangular (*a/b*=2) planform. The panel thickness is kept constant for *h/a*=0.01, and the degree of curvature is taken as *a/R*=0 (plate), 0.2 (relatively shallow) and 0.5 (relatively deep) in the examples. A rise of the center is only 3 percent of the radius *R* for a shell of *a/R*=0.5, and this can be regarded as geometry within the *shallow* shell theory. The range of applicability of the shallow shell theory is given, for example [24], in detail. The elastic constants used are for a Graphite/epoxy composite and have the values of E_L= 138 GPa, E_T=8.96 GPa , G_{LT}=7.1 GPa and ν_{LT}=0.30.

The design variables are presented in the usual notation as $[\theta_1/\theta_2/\theta_3/\theta_4]_s$, where θ_1 is the fiber orientation angle of the 1st layer (outermost) and θ_4 is that of the 4th layer (innermost). The out-of-plane boundary conditions are given for free (F), simply supported (S) and clamped (C) edges, and the corresponding in-plane boundary conditions to the F, S and C notations are defined as in Eq.(20). The letters F,S and C are used in combination to express the edge support conditions along the edges at *x=-a/2*, *y=-b/2*, *x=a/2* and *y= b/2* in this order, i.e. in a counterclockwise order starting with Edge(1) (See Fig.1).

To demonstrate the accuracy of the vibration solutions, a convergence study is presented in Table 1 for the lowest four frequency parameters $\Omega_1 \sim \Omega_4$ of the square panel with a typical lay-up $[30/-30/30/-30]_s$. (For brevity, the fiber angles in brackets [ ] are denoted by the number, i.e., 30 instead of 30° in this paper). The lowest four frequencies presented for the SSSS and CCCC panels show rapid convergence rates, monotonically decreasing from above, as the number of terms, $M \times N$, in each displacement of Eq.(16) is increased from 6×6 to 12×12. The fundamental frequency Ω_1 is converged within the four significant figures for the 10×10 solutions (converged values in the table are underlined), and this number of terms is used in evaluating the object functions in the present optimization. The determinant size in the eigenvalue problem therefore becomes 300×300, i.e. $10 \times 10 \times 3=300$ for the three displacements *u, v* and *w*.

Tab.1

Table 2 shows that for typical FFFF, SSSS and CCCC panels vibration analysis performed for this paper is in good agreement with the other published results; for the angle-ply and cross-ply 4-layer panels (FFFF, CCCC) the frequency parameter values are in close agreement [9,14], and for the cross-ply 12-layer panel (SSSS) the results are identical to the exact values [18]. The vibration solution accuracy is therefore well established.

Tab.2

In order to demonstrate the effectiveness of the LO procedure in determining the lay-ups which maximize the fundamental frequency of laminated panels, one example is presented in Table 3. This deals with symmetrically laminated 8-layer rectangular panel (a/b=2, a/R=0.5) with SSSS boundary condition. In applying the iterative LO procedure to an 8-layer panel, the upper (lower) four layers are assumed first (Step 0) to be hypothetical layers with no rigidity. In Step 1, the first (outermost) layer is replaced by an orthotropic CFRP layer with given elastic properties and the optimum fiber orientation angle $\theta_{1,opt}$ is determined sequentially by changing θ_1 in 5° increments starting from -90° and finishing at +90°. (Finer increments may be used depending on the desired solution accuracy.) In Step 2, $\theta_{2,opt}$ is determined for a panel with the fiber angle of the first layer maintained at $\theta_{1,opt}$ and the virtual second layer is replaced by an orthotropic CFRP layer. This process is terminated after $\theta_{4,opt}$ is determined in Step 4. The first set of solutions $[\theta_1/\theta_2/\theta_3/\theta_4]_{s,opt}$ is then used as an initial approximation of the solution for a second iterative cycle of the LO procedure [21]. In Table 3, Step 4 of the second iterative cycle gives $[40/-45/-45/-45]_S$ and the third iterative cycle gives an identical set of fiber

Tab.3

orientation angles as those resulting from the second iterative cycle, signifying a converged design.

Table 4 presents converged optimum solutions for symmetric 8-layer square panels with various combinations of F, S and C. The maximized fundamental frequencies Ω_{opt} (Subscript "1" in $\Omega_{1,opt}$ is omitted hereafter for simplicity) are given for *a/R*=0.2 and 0.5, each for ten different sets of boundary conditions, together with the optimum fiber orientation angles and the number of iterative cycles (NIC) required to obtain the converged results. In the majority of cases presented here, converged or optimum lay-ups are determined after more than one iterative cycle of the LO procedure. It may be noted that the FFFF panel yields higher optimum frequency than the CFFF, FCFF, CSFF, SCFF and CCFF panels that have more edge constraints. This is because the FFFF panel shows rigid body motions (note that the present eigenvalue calculation yields zero eigenvalues for FFFF panel due to the general nature of displacement function including m=0 and n=0) and the lowest elastic vibration mode has higher frequency values than these panels.

Tab.4

Comparisons are made in Fig.3 and Fig.4 to demonstrate that the panels with the present optimum lay-ups $[\theta_1/\theta_2/\theta_3/\theta_4]_{s,opt}$ actually give higher fundamental frequencies than panels with other stacking sequences. Typical stacking sequences of symmetric 8-layer panels are chosen for comparison purposes, namely [0/0/0/0]s, [90/90/90/90]s, [30/-30/30/-30]s, [60/-60/60/-60]s [45/-45/45/-45]s and [0/-45/45/90]s. The first two (i.e., $[0_4]$s are $[90_4]$s) are specially orthotropic and the higher fundamental frequency of these two lay-ups is presented for clarity of the figure and denoted by ◆ in the figure. Similarly, the higher fundamental frequency is presented in the figure for the two alternating angle-ply sequences, $[(30/-30)_2]$s and $[(60/-60)_2]$s and is denoted by ◇. The $[(45/-45)_2]$s is an alternating angle-ply lay-up, which is diagonally orthotropic for square panels, and is denoted by ▲. The last one ([0/-45/45/90]s) is a quasi-isotropic lay-up, denoted by △. It is observed that all of the present optimum solutions (denoted by ■) have higher fundamental frequencies than the panels with the six typical lay-ups without exception.

Fig.3

Fig.4

Table 5 presents converged optimum solutions for symmetric 8-layer *rectangular* (*a/b*=2) panels with various combinations of F, S and C. The maximized fundamental frequencies Ω_{opt} are given again for *a/R*=0.2 and 0.5, each for ten different sets of boundary conditions, together

Tab.5

with the optimum fiber orientation angles and the number of iterative cycles. The optimum lay-ups are normally determined, as for square panels, after more than one iterative cycle of the LO procedure, and NIC=2 is found for all the cases of a/R=0.5 with only one exception. The comparison of the optimum panel frequencies with those of typical lay-ups, as shown in Fig.3 and Fig.4 for a square panel, was also performed for the rectangular panel. All of the present optimum solutions were found to have higher fundamental frequencies than the panels with the six typical lay-ups without exception (but not presented here due to space limitation).

The accuracy of the LO procedure is thus demonstrated in Figs.3 and 4 by comparing to the fundamental frequencies of plates with typical lay-ups, but this is not mathematical proof for the global optimum. Therefore in the last example, the global solutions were calculated for all the combinations of 36^4 in the discrete angles of θ=5 in two specific cases, although it was excessively time consuming. The boundary condition and a value of a/R were chosen randomly, one from cases in Table 4 and one from Table 5.

Table 6 presents the highest ten fundamental frequencies for the 8-layer panels obtained in this numerical experiment. The results are given for a square panel with large curvature (a/b=1, a/R=0.5) and a rectangular panel with small curvature (a/b=2, a/R=0.2) in (a) and (b), respectively. For the square panel with SCFF boundaries in (a), the LO solution (given in a thick frame) is listed in the 27th place (within the top 0.0016 percent) among 36^4 combinations. In (b), where a simply supported panel (SSSS) is considered, the LO solution is located in the 4th place. It is interesting to know in both (a) and (b) that the differences between the global solution and LO solution are the same, 0.08 percent, regardless of the rank. Thus the advantage is significant when one considers a significantly short computation time of the LO approach, and the LO approach gives remarkably accurate solutions to the global optimum among almost innumerable combinations.

5 CONCLUSIONS

It has been established that the Ritz method with special displacement functions performs well for calculating the natural frequencies of laminated curved panels with general edge conditions, and can be implemented in the layerwise optimization procedure which was recently proposed for flat plate optimization. The optimum lay-ups for the maximum fundamental

frequencies are determined by the combination of the analysis method and the optimization procedure, and it is numerically demonstrated that the present optimum fundamental frequencies are actually higher than curved panels with any of typical lay-ups and are almost equivalent to the global solutions.

Acknowledgements

The first author wishes to express his appreciation to Prof. F.L.Matthews, former Director of the Composites Centre, Imperial College London, for his acceptance as an academic visitor and also to the financial support from the Japan Society for the Promotion of Science (JSPS).

REFERENCES

[1] Leissa, AW. Vibration of Shells. *US Government Printing Office* 1973, reprinted in 1993 by The Acoustical Society of America.

[2] Qatu MS. Review of shallow vibration research. *Shock and Vibr Dig* 1992; 24: 3-5.

[3] Liew KM, Lim CM, Kitipornchai S. Various theories for vibration of shallow shells: a review with bibliography. *Appl Mech Rev* 1997; 50: 431-444.

[4] Leissa AW, Qatu MS. Equations of elastic deformation of laminated composite shallow shells. *ASME Jnl Appl Mech* 1991; 58: 181-188.

[5] Bert CW, Kumar M, Vibration of cylindrical shells of bimodulus composite materials. *Jnl Sound Vibr* 1982; 81: 107-121.

[6] Soldatos KP, A comparison of some shell theories used for the dynamic analysis of cross-ply laminated circular cylindrical panels. *Jnl Sound Vibr* 1984; 97: 305-319.

[7] Soldatos KP, Influence of thickness shear deformation on free vibrations of rectangular plates, cylindrical panels and cylinders of antisymmetric angle-ply construction. *Jnl Sound Vibr* 1987; 119: 111-137.

[8] Lam KY, Chun L. Dynamic analysis of clamped laminated curved panels. *Compo Struct* 1995; 30: 389-398.

[9] Berçin, AN. Natural frequencies of cross-ply laminated singly curved panels. *Mech Res Comm* 1996; 23: 165-170.

[10] Bardell NS, Dunsdon JN, Langley RS. Free and forced vibration analysis of thin, laminated, cylindrically curved panels. *Compo Struct* 1997; 38: 453-462.

[11] Selmane A, Lakis AA. Dynamic analysis of anisotropic open cylindrical shells. *Compu Struct* 1997; 62: 1-12.

[12] Soldatos KP, Messina A. The influence of boundary conditions and transverse shear on the vibration of angle-ply laminated plates, circular cylinders and cylindrical panels. *Comp Methods Appl Mech Engng* 2001; 190: 2385-2409.

[13] Kabir, HRH. Application of linear shallow shell theory of Reissner to frequency response of thin cylindrical panels with arbitrary lamination. *Compo Struct* 2002; 56: 35-52.

[14] Zhao X, Liew KM, Ng TY. Vibration analysis of laminated composite cylindrical panels via a meshfree approach. *Int Jnl of Solids Struct* 2003; 40: 161-180.

[15] Raouf, RA. Tailoring the dynamic characteristics of composite panels using fiber orientation. *Compo Struct* 1994; 29: 259-267.

[16] Narita Y, Itoh M, Zhao X. Optimal design by genetic algorithm for maximum fundamental frequency of laminated shallow shells. *Adv Compo Lett* 1996; 5: 21-24.

[17] Narita Y, Zhao X. An optimal design for the maximum fundamental frequency of laminated shallow shells. *Int Jnl Solids Struct* 1998; 35: 2571-2583.

[18] Narita Y, Nitta T. Optimal design by using various solutions for vibration of laminated shallow shells on shear diaphragms. *Jnl Sound Vibr* 1998; 214: 227-244.

[19] Narita Y. Combinations for the free-vibration behaviors of anisotropic rectangular plates under general edge conditions. *ASME Jnl Appl Mech* 2000; 67: 568-573.

[20] Narita Y. Layerwise optimization for the maximum frequency of laminated composite plates. *Jnl Sound Vibr* 2003; 263: 1005-1016.

[21] Narita Y, Hodgkinson JM. Layerwise optimization for maximising the fundamental frequencies of point-supported rectangular laminated composite plates. *Compo Struct* 2005; 69: 127-135.

[22] Vinson JR, Sierakowski RL. *The Behavior of Structures Composed of Composite Materials*, Martinus Nijhoff, Dordrecht, 1986.

[23] Jones RM. *Mechanics of Composite Materials- 2nd ed*., Taylor & Francis, Inc. 1999.

[24] Lee JK, Leissa AW, Wang AJ. Vibrations of cantilevered circular cylindrical shells: shallow versus deep shell theory. *Int. J. Mech. Sci*., 1983; 25: 361-383.

(Figure and table Captions)

Fig.1 Mid-surface of cylindrically curved panel.

Fig.2 Flow chart of the algorithm used in the LO approach.

Fig.3 Comparison between the optimum frequency parameter $\Omega_{1,opt}$ and frequency parameters for a symmetric 8-layer cylindrical square panel for various lay-ups, (*a/b*=1, *a/R*=0.2).

Fig.4 Comparison between the optimum frequency parameter $\Omega_{1,opt}$ and frequency parameters for a symmetric 8-layer cylindrical square panel for various lay-ups, (*a/b*=1, *a/R*=0.5).

Table 1 Convergence study of frequency parameters for symmetrically laminated, 8-layer cylindrical square panels (*a/b*=1, *h/a*=0.01, *a/R*=0.5, [30/-30/30/-30]s).

Table 2 Comparison of frequency parameters for symmetrically laminated cylindrical square panels (*a/b*=1, *h/a*=0.01).

Table 3 Illustration of the LO procedure for a symmetrically laminated, 8-layer rectangular panel (*a/b*=2, *a/R*=0.5, SSSS panel, Increment is θ=5°).

Table 4 Converged optimum solutions by a LO procedure for symmetrically laminated, 8-layer square panels with various boundary conditions (*a/b*=1, Increment is θ=5°).

Table 5 Converged optimum solutions by a LO procedure for symmetrically laminated, 8-layer rectangular panels with various boundary conditions (*a/b*=2, Increment is θ=5°).

Table 6 Comparison of the LO solutions with the global solutions for symmetrically laminated, 8-layer cylindrical panels (*h/a*=0.01, Increment is 5°).

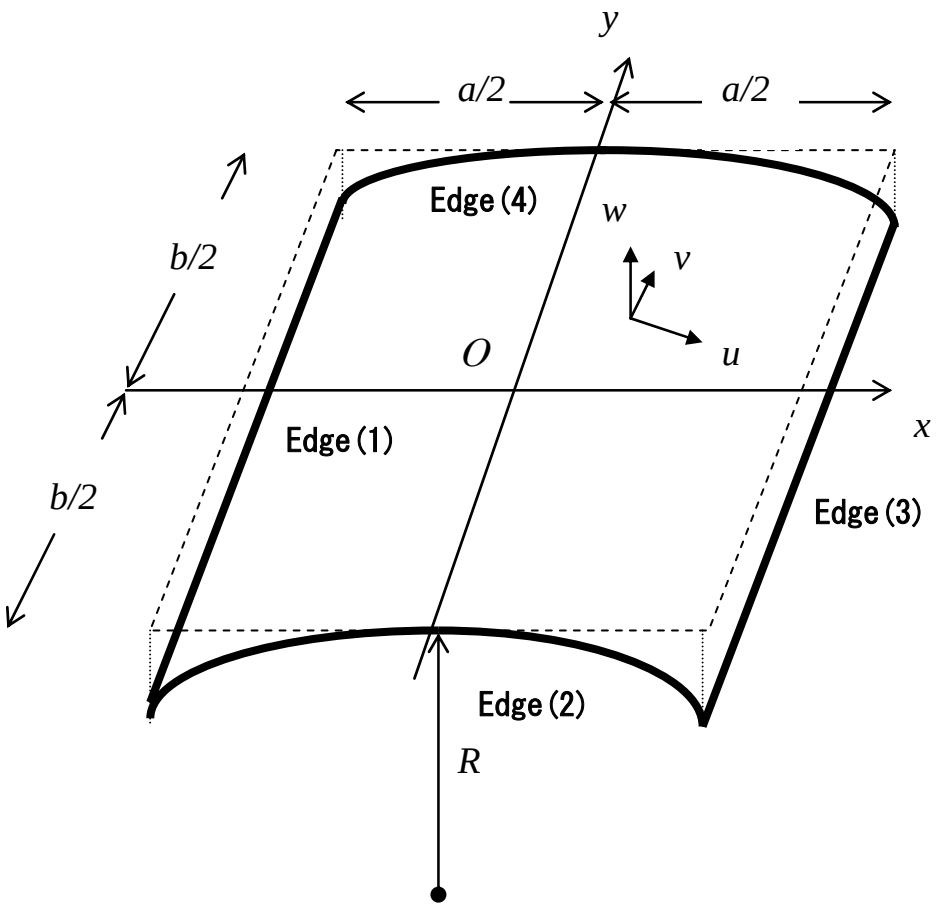

Fig.1 Mid-surface of cylindrically curved panel

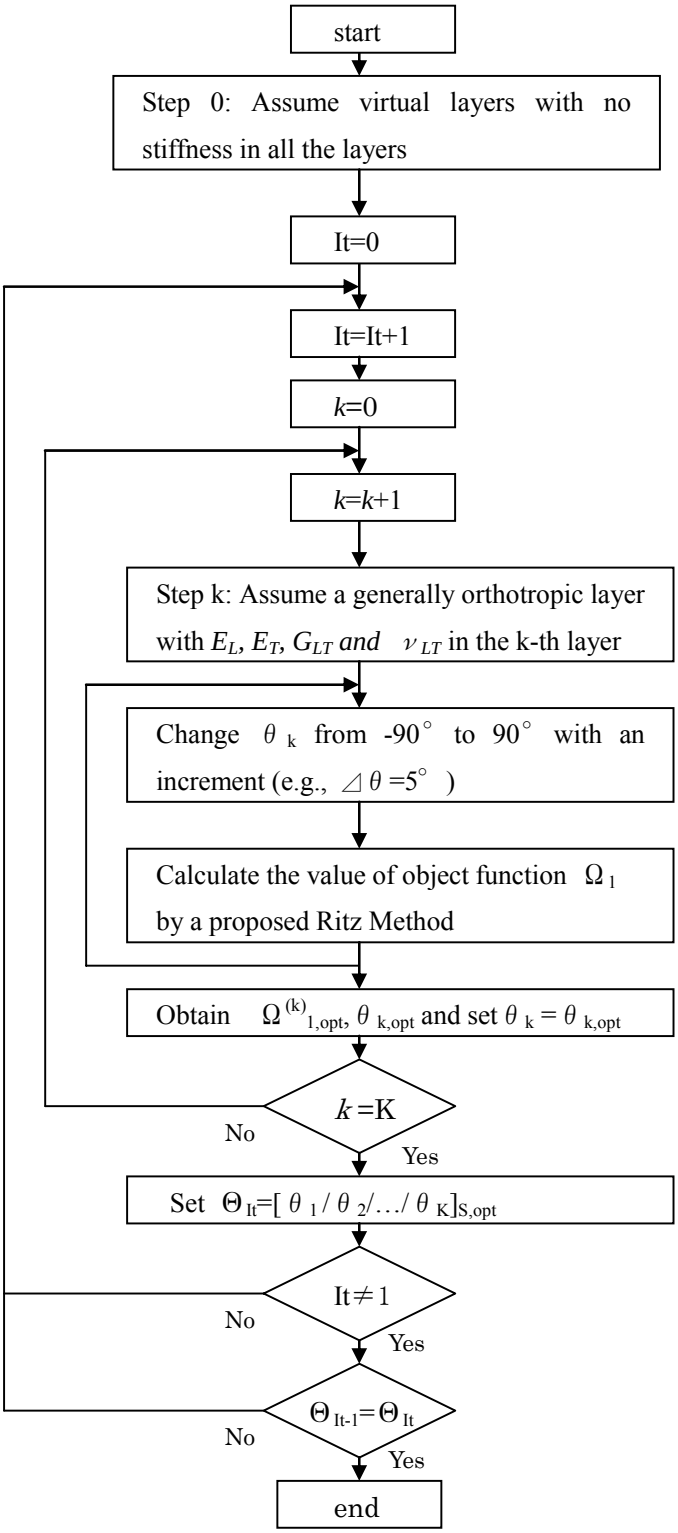

Fig.2 Flow chart of the algorithm used in the LO approach

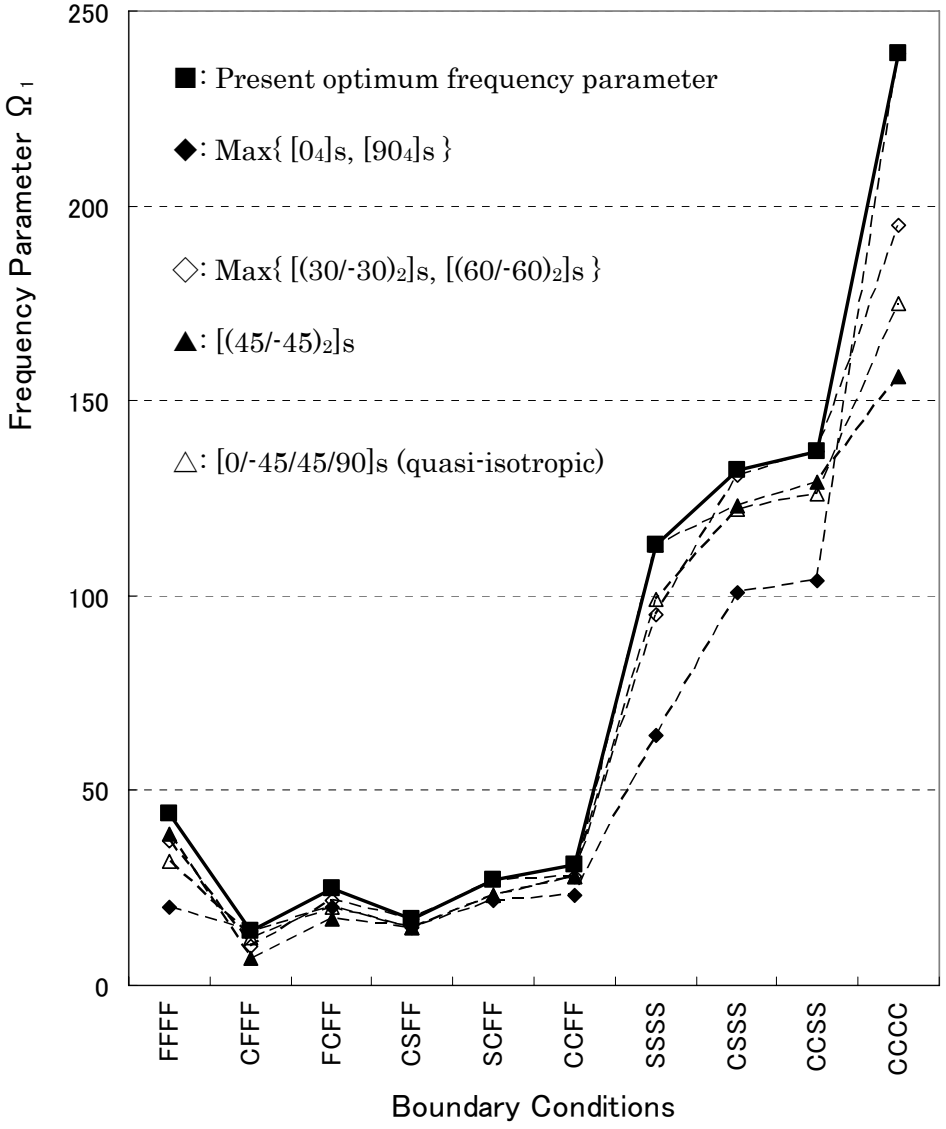

Fig.3 Comparison between the optimum frequency parameter $\Omega_{1,opt}$ and frequency parameters for a symmetric 8-layer cylindrical square panel for various lay-ups, (a/b=1, a/R=0.2).

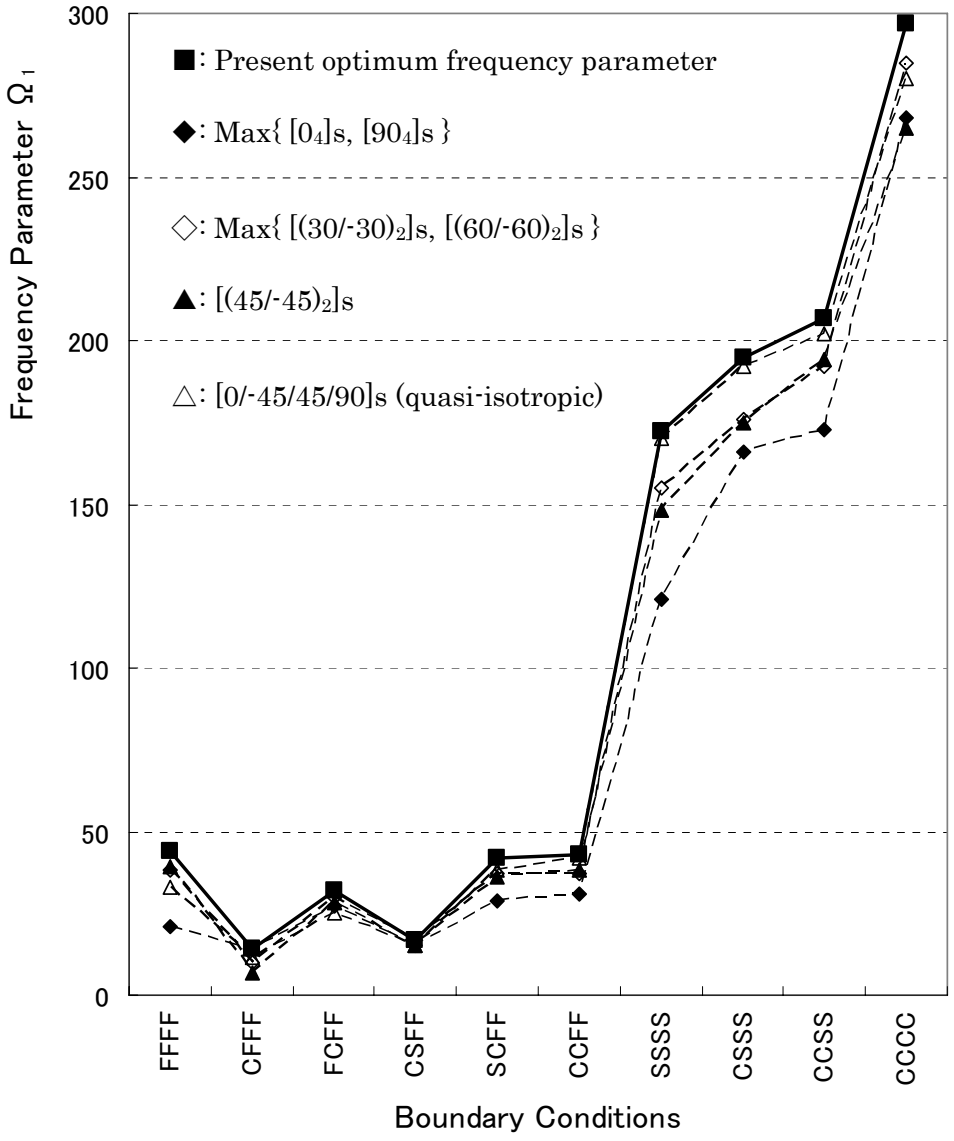

Fig.4 Comparison between the optimum frequency parameter $\Omega_{1,opt}$ and frequency parameters for a symmetric 8-layer cylindrical square panel for various lay-ups, (a/b=1, a/R=0.5).

Table 1 Convergence study of frequency parameters for symmetrically laminated, 8-layer cylindrical square panels ($a/b=1$, $h/a=0.01$, $a/R=0.5$, [30/-30/30/-30]s)

$M \times N$	Ω_1	Ω_2	Ω_3	Ω_4
SSSS panel				
6 × 6	160.0	200.3	286.3	316.2
8 × 8	154.9	200.3	280.6	305.0
10 × 10	154.8	200.3	280.5	304.7
12 × 12	154.8	200.3	280.5	304.7
CCCC panel				
6 × 6	285.4	349.3	420.0	429.8
8 × 8	284.6	348.5	419.0	429.3
10 × 10	284.6	348.5	419.0	429.3
12 × 12	284.6	348.5	419.0	429.3

Table 2 Comparison of frequency parameters for symmetrically laminated cylindrical square panels (a/b=1, h/a=0.01)

	Ω_1	Ω_2	Ω_3	Ω_4
FFFF panel (4 layers)*				
$[30/-30]_S$	30.03	69.45	75.46	104.1
Ref.[14]	30.11	69.30	75.33	104.2
SSSS panel (12 layers)*				
$[(0/90)_3]_S$	146.4	147.5	226.0	280.7
Ref.[18]	146.4	147.5	226.0	280.7
mode	(1,1)	(2,1)	(2,2)	(1,2)
CCCC panel (4 layers)**				
$[0/90]_S$	188.4	217.7	239.3	277.7
Ref.[9]	188.3	217.7	239.3	277.7
$[30/-30]_S$	191.8	207.6	236.2	266.2
Ref.[14]	191.8	207.6	236.1	266.3

*: The same elastic constants as used in the present study, and a/R=0.5

**: E_L/E_T=15.4, G_{LT}/E_T=0.8, ν_{LT}=0.3 and a/R=0.2

Table 3 Illustration of the LO procedure for a symmetrically laminated, 8-layer rectangular panel (a/b=2, a/R=0.5, SSSS panel, Increment is θ=5°)

Present	$[\theta^{(1)}/\theta^{(2)}/\theta^{(3)}/\theta^{(4)}]_s$	Ω_{opt}
1st iterative cycle of solutions		
Step 0	[∗/∗/∗/∗]s	–
Step 1	[35/∗/∗/∗]s	158.2
Step 2	[35/−45/∗/∗]s	263.9
Step 3	[35/−45/50/∗]s	299.2
Step 4	[35/−45/50/−45]s	328.2
2nd iterative cycle of solutions		
Step 0	[35/−45/50/−45]s	328.2
Step 1	[40/−45/50/−45]s	328.8
Step 2	[40/−45/50/−45]s	328.8
Step 3	[40/−45/−45/−45]s	330.2
Step 4	[40/−45/−45/−45]s	330.2
3rd iterative cycle of solutions (same as 2nd)		330.2

Table 4 Converged optimum solutions by a LO procedure for symmetrically laminated, 8-layer square panels with various boundary conditions (a/b=1, Increment is θ=5°)

B.C.	$[\theta_1/\theta_2/\theta_3/\theta_4]_{s,opt}$	Ω_{opt}	NIC*
a/R =0.2			
FFFF	[45/−40/−40/−45]s	43.59	2
CFFF	[0/0/0/0]s	13.76	1
FCFF	[70/−60/−70/80]s	24.67	2
CSFF	[20/25/−45/−10]s	16.91	3
SCFF	[60/−55/−80/−85]s	27.28	2
CCFF	[35/−40/−85/90]s	30.61	3
SSSS	[45/−45/45/−45]s	113.4	1
CSSS	[20/−30/40/−35]s	131.9	2
CCSS	[35/−30/35/−30]s	137.1	1
CCCC	[0/0/0/0]s	239.4	1
a/R =0.5			
FFFF	[45/−40/−40/−40]s	43.83	2
CFFF	[0/0/0/0]s	13.63	1
FCFF	[55/−50/−85/90]s	32.02	3
CSFF	[25/20/20/−25]s	17.05	2
SCFF	[25/−50/80/−85]s	41.50	3
CCFF	[25/−40/85/−85]s	43.43	4
SSSS	[5/0/−45/75]s	172.3	4
CSSS	[5/−25/50/−65]s	194.5	3
CCSS	[5/−40/50/60]s	206.9	3
CCCC	[5/−20/40/−45]s	296.8	2

*NIC: Number of Iterative Cycle

Table 5 Converged optimum solutions by a LO procedure for symmetrically laminated, 8-layer rectangular panels with various boundary conditions (a/b=2, Increment is θ=5°)

B.C.	$[\theta_1/\theta_2/\theta_3/\theta_4]_{s,opt}$	Ω_{opt}	NIC*
a/R =0.2			
FFFF	[5/−40/50/50]s	65.61	2
CFFF	[0/0/0/0]s	13.78	1
FCFF	[85/−85/−55/50]s	66.12	2
CSFF	[35/−40/−45/−45]s	26.16	3
SCFF	[75/75/−55/20]s	71.88	3
CCFF	[75/85/35/−45]s	71.48	2
SSSS	[75/−50/25/−15]s	202.5	3
CSSS	[60/−50/15/−5]s	209.4	3
CCSS	[90/−85/40/−15]s	268.1	3
CCCC	[90/90/90/0]s	374.2	2
a/R =0.5			
FFFF	[5/−40/45/45]s	65.81	2
CFFF	[0/0/0/5]s	13.63	1
FCFF	[85/90/−45/45]s	83.04	2
CSFF	[35/−40/−40/30]s	25.60	2
SCFF	[70/40/−50/−85]s	91.28	2
CCFF	[60/−55/35/90]s	92.29	2
SSSS	[40/−45/45/−45]s	330.2	2
CSSS	[35/−40/45/−45]s	342.9	2
CCSS	[45/−45/30/−35]s	373.8	2
CCCC	[85/−40/30/−25]s	447.9	2

*NIC: Number of Iterative Cycle

Table 6 Comparison of the LO solutions with the global solutions for symmetrically laminated, 8-layer cylindrical panells (h/a =0.01, Increment is 5°).

(a) SCFF (a/b =1, a/R =0.5)			(b) SSSS (a/b =2, a/R =0.2)		
rank	Ω_{opt}	$[\theta_1/\theta_2/\theta_3/\theta_4]$s	rank	Ω_{opt}	$[\theta_1/\theta_2/\theta_3/\theta_4]$s
1	17.061	[25/20/20/−15]s	1	202.68	[75/−50/30−10]s
−	17.061	[20/25/20/−15]s	2	202.65	[75/−50/30/−5]s
3	17.059	[25/20/20/−20]s	3	202.58	[80/−50/30/−10]s
−	17.059	[20/25/20/−20]s	4	202.52	[75/−50/25/−15]s
5	17.058	[25/20/25/−25]s	5	202.49	[75/−50/30/0]s
−	17.058	[20/25/25/−25]s	−	202.49	[75/−50/25/−10]s
7	17.056	[25/20/20/−30]s	7	202.48	[80/−50/35/−5]s
−	17.056	[20/25/20/−30]s	−	202.48	[75/−50/30/−15]s
−	17.056	[20/20/25/−30]s	−	202.48	[80/−50/30/−15]s
10	17.054	[25/20/15/−25]s	10	202.47	[80/−50/30/−5]s
27	17.048	[25/20/20/−25]s			

: LO solution